

# Development of reversible glutamine conjugate of methotrexate for enhanced brain delivery

Vijay Kumar Singh · Bharat Bhusan Subudhi

Received: 15 February 2014 / Accepted: 6 July 2014 / Published online: 20 July 2014  
© Springer Science+Business Media New York 2014

**Abstract** Poor permeability of methotrexate across blood brain barrier limits its scope for application against brain cancer. Glutamine is transported to brain actively by multiple amino acid transporters and protects against complications of chemotherapy. To use glutamine as a carrier, a reversible conjugate of methotrexate was developed with structural features of glutamine. This was stable and released methotrexate effectively. The brain uptake was enhanced significantly

**Keywords** Glutamine · Methotrexate · Conjugate · Brain

## Introduction

Methotrexate (MTX), as a folate antagonist, has been widely used in many form of cancer. However, it is not effective against brain tumours like many other anticancer agents. This is because of its inability to cross blood brain barrier. Although it is believed to be transported by reduced folate carrier, limited capacity of this transporter is unable to ensure enough bioavailability for any therapeutic utility against brain tumour. Very high (1–8 g/m<sup>2</sup>) doses may enhance brain availability, but being a folate antagonist at these dose level, it becomes too toxic for any

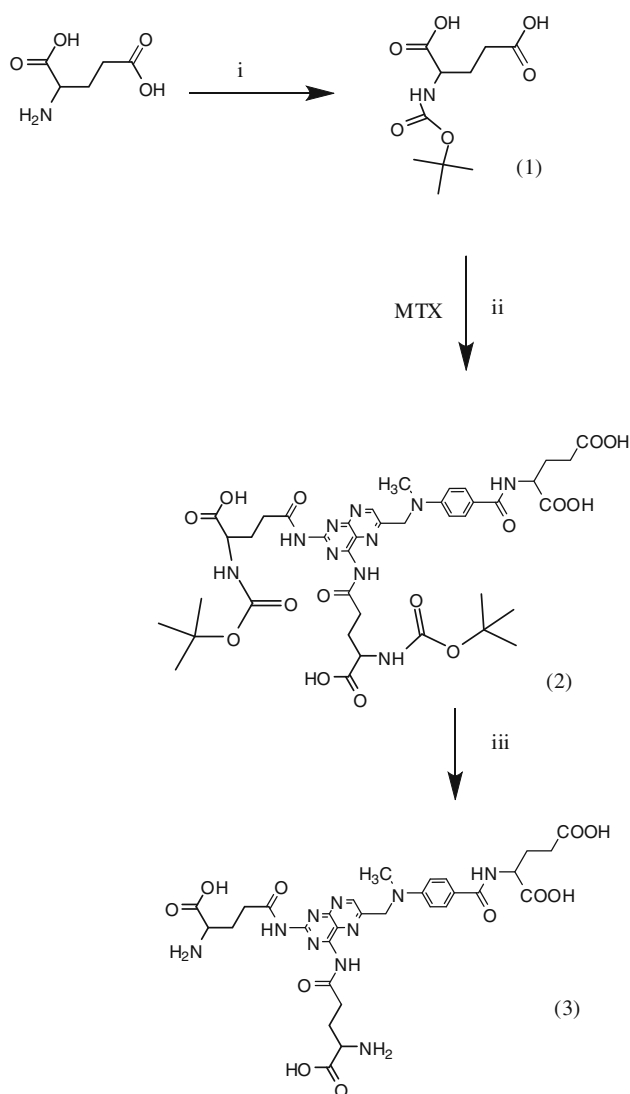
practical use (Batchelor *et al.*, 2003; De Angelis *et al.*, 2002; O'Brien *et al.*, 2000; Holmboe *et al.*, 2012; Widemann and Adamson 2006). This makes chemotherapy against brain tumour ineffective. So, there is major challenge to enhance brain availability of MTX to increase its therapeutic utility.

To address this, many attempts have been made including development of cetuximab (IMC-C225) dendrimer bioconjugates, osmotic blood–brain barrier disruption, intracarotid administration of short-chain alkylglycerols and transnasal delivery (Erdlenbruch *et al.*, 2003; Neuwelt *et al.*, 1981; Shingaki *et al.*, 2010; Wu *et al.*, 2006). However, these approaches, so far have not been able to provide an ideal solution and there is scope for evaluation of other approaches to enhance its brain delivery.

Endogenous amino acid transportation systems exist in BBB for brain transport of amino acids for normal functioning of brain. These transportation systems can be capitalised for brain transportation of drugs provided they meet some structural necessity of their substrates. Accordingly, there have been reports of prodrug/co-drug that permeates BBB by mimicking as substrates (Gabathuler, 2010; Pardridge, 2012; Peura *et al.*, 2013). Chemically, MTX is *N*-[4-[(2,4-diamino-6-pteridinyl) methyl] methylamino] benzoyl]-L-glutamic acid. However, glutamic acid moiety is a poor carrier as transport capacity for anionic amino acid system (system x<sub>G</sub><sup>-</sup>) is quite low compared to neutral amino acids (Al-Sarraf *et al.*, 1995, 1997a, b; Drewes *et al.*, 1977; Hawkins *et al.*, 1995). Unlike glutamic acid, its amide glutamine (GLU) is a good substrate for large neutral amino acid transporter L1 (LAT1). This transport system is the most important source by which essential amino acids gain access to the brain and it has capacity to transport relatively larger molecule provided they meet the basic structural feature including free

V. K. Singh  
Columbia Institute of Pharmacy, Raipur 493111, Chhatisgarh,  
India  
e-mail: vijaysingh1207@gmail.com

B. B. Subudhi (✉)  
School of Pharmaceutical Sciences, Siksha O Anusandhan  
University, Bhubaneswar 751003, Orissa, India  
e-mail: bharatbhusans@gmail.com



**Scheme 1** Synthesis of MTX-GLU. (i) Et<sub>3</sub>N, THF, (BOC)<sub>2</sub>O (ii) CH<sub>2</sub>Cl<sub>2</sub>, DMAP, DCC (iii) 4 N HCl, 1,4 Dioxane

$\alpha$ -amino and carboxyl group (Uchino *et al.*, 2002; Hawkins *et al.*, 2006; Geiera *et al.*, 2013). This has been capitalised for transport of drugs to brain (Bauwens *et al.*, 2007; Hellwig *et al.*, 2008; Kersemans *et al.*, 2005; Gabathuler, 2010; Pardridge, 2012; Peura *et al.*, 2013). Additionally, Na-dependent glutamine transporters (systems A and N) also facilitate permeation of glutamine across BBB (Ennis *et al.*, 1998). Besides, glutamine is also a substrate to other amino acid transporters expressed at BBB including ATB<sup>0,+</sup> (Umaphathy *et al.*, 2008; Czeredys *et al.*, 2008). Thus, these multiple transportation systems may help transportation of glutamine conjugate of MTX across BBB to deliver MTX in brain. Glutamine is also known to reduce complications of chemotherapy including cytotoxicity and neurotoxicity (Stubblefield *et al.*, 2005; Gourav *et al.*, 2012). Taking these facts into consideration, we tried

to use structural features of glutamine and developed reversible conjugate with MTX (MTX-GLU) to improve its brain permeability.

## Results and Discussion

### Chemistry

We prepared 2-(4-(((2, 4-bis (2-amino-4-carboxybutanamido) pteridin-6-yl) methyl) (methyl) amino) benzamido) pentanedioic acid (3) as per Scheme 1. Synthesis was done following reported method with some modification (Laulloo *et al.*, 2007; Martin *et al.*, 2002). The starting material was glutamic acid. The  $\alpha$ -amino group of glutamic acid was protected so as to prevent its competition for amide formation in the last step of reaction. This was done with the formation of t-Boc group with amine. As glutamic acid contains two carboxylic acid groups, in the subsequent reaction, both may compete for activation with DCC. To avoid this, pH was controlled around 3 so that the  $\alpha$ -carboxylic acid groups (pKa, 2) remain ionised and do not participate where as the side chain carboxylic acid (pKa, 4.5) largely becomes free for activation. Under this condition, glutamic acid was activated and added to MTX leading to formation of the compound 2. The t-Boc group was finally removed to yield 3 (MTX-GLU). This ensures free  $\alpha$ -amino and carboxyl group in the structure, as desirable for substrate specificity of LAT1. Considering the close nucleophilicity of both amino groups present in MTX, two amide bonds are formed with GLU. This is evident from the mass spectrum of MTX-GLU with molecular ion (M+1) peak at 713.32. This was further supported by the <sup>13</sup>C NMR, <sup>1</sup>H NMR and FTIR peaks as assigned in the experimental section. Elemental analysis of MTX-GLU was in close agreement with the calculated values and confirmed the proposed structure.

### Analytical method

The chromatographic separations were achieved on a promocil C18 column (4.6 mm  $\times$  250 mm, 5  $\mu$ m), thermostated at 27  $^{\circ}$ C. The solvent system comprised phosphate buffer (10 mmol dihydrogen phosphate and 10 mmol sodium hydroxide, pH 7.4) premixed, filtered and degassed in water: methanol: acetonitrile (70:20:10) at a flow rate of 1 ml/min. The retention time of MTX-GLU was 6.4 min (295 nm) and that of MTX was 7.3 min (310 nm). The method was validated before use as per the ICH guidelines. Calibration curves displayed good linearity ( $r > 0.998$ ) within the tested concentration ranges. The recovery range and the relative standard deviation for each of the analytes

were found to be 95.68–99.82 and 0.324–0.776 %, respectively.

#### Stability of MTX–GLU in buffers

To characterise chemical stability, it was incubated in pH 2.0, 4.9, 7.4 and 8.0 phosphate buffers. The pseudo first-order rate constants ( $K_{\text{disapp}}$ ) and half life ( $t_{1/2}$ ) are shown in Table 1. MTX–GLU appeared to be stable in pH 7.4 phosphate buffer and moderately stable at other pH. The slow hydrolysis at pH 7.4 indicated its ability for sustained release in physiological conditions. MTX–GLU in this condition, for practical purposes can be considered as stable for further evaluation.

#### Stability in plasma and brain

For a prodrug expected to reach brain must survive plasma transportation. MTX–GLU with amide bonds is expected to be slowly hydrolysed in plasma (Rao *et al.*, 1987; Simoes *et al.*, 2009). Accordingly, the prodrug exhibited  $K_{\text{disapp}}$  value of  $3.11 \times 10^{-3}$  min. This was faster than the degradation rate in pH 7.4 phosphate buffer suggesting contribution of enzymes in plasma to the degradation of prodrug. However, in spite of this, stability in plasma can be considered reasonable to give enough time ( $t_{1/2} = 229.17 \pm 6.37$  min) for distribution to brain. In brain homogenate, it degraded with a higher rate (Table 2). Similar observation of higher degradation in brain has been reported in a recent work suggesting involvement of relatively higher metabolism and other process that reduce drug level (Zhou *et al.*, 2013). However, the degradation of

prodrug in brain can be considered slow enough ( $t_{1/2} = 128.70 \pm 1.27$  min) to favour a sustained action.

#### Distribution coefficients and protein binding

The limited access MTX to brain is partly attributed to its poor distribution coefficient because of polar nature. Accordingly, octanol–water distribution coefficient ( $\log D$ ) in buffered solution at pH 7.4 at room temperature was determined for MTX–GLU. A  $\log D$  value of  $-1.78$  for MTX–GLU indicated its polar nature. Conjugation to GLU seems to have not altered the  $\log D$  significantly (Table 3). This may be because of the fact that even though it masks two amine groups of MTX, it also adds polar groups to the molecule.

Binding to plasma proteins strongly influences the entry of drugs into the central nervous compartments as in the presence of an intact barrier, only the plasma fraction unbound can freely penetrate (Norrby, 1985). The in vitro plasma protein binding study revealed that 38–43 % MTX were in bound form. This is in agreement with a previous study that showed plasma protein binding in the range of 25–55 % (Combe *et al.*, 1995). The prodrug exhibited 35–43 % of plasma protein binding (Table 3). This suggests that both MTX and MTX–GLU exhibit comparable protein binding and in general this level of binding can be considered reasonable for transport.

#### In vitro release of MTX in brain homogenate

To study the release of MTX by the prodrug, peak corresponding to MTX was analysed. The data suggest that MTX was released from the prodrug steadily in brain homogenate (Fig. 1). The release of MTX is assumed to be by cleavage of amide bond. Other than the two amide bonds produced by synthesis, MTX itself contains one amide bond. The appearance of peak corresponding to standard MTX in HPLC shows that MTX is intact and only those two bonds of prodrug with GLU have undergone degradation. Besides hydrolysis of MTX at the amide bond is a very minor route of MTX metabolism as only less than 5 % of the drug gets eliminated in this form (Donehower *et al.*, 1979; Widemann *et al.*, 2000). However, it needs further investigation to find out the pattern of enzymatic degradation for MTX–GLU.

The release was observed to be slow ( $K_{\text{app}}$ ,  $2.91 \times 10^{-3}$  min). In contrast to disappearance of MTX–GLU ( $K_{\text{disapp}} = 5.38 \times 10^{-3}$  min), release of MTX was found to be less. This can be attributed to other degradation routes that do not result in MTX. However, the slow release can sustain the effects of MTX which may be beneficial in treatment tumours that generally require a prolonged exposure (Ozeki *et al.*, 2010). As the above

**Table 1** Stability studies in different buffer solutions

Compound	pH value	Kinetic constant	
		$K$ ( $\text{h}^{-1}$ )	$t_{1/2}$ (h)
MTX–GLU	2.0	$5.42 \times 10^{-2}$	$12.77 \pm 0.25$
	4.9	$3.90 \times 10^{-2}$	$17.71 \pm 0.21$
	7.4	$1.30 \times 10^{-2}$	$52.88 \pm 0.90$
	8.0	$2.17 \times 10^{-2}$	$31.87 \pm 0.14$

$n = 3$

**Table 2** Stability in plasma extracts and brain homogenate

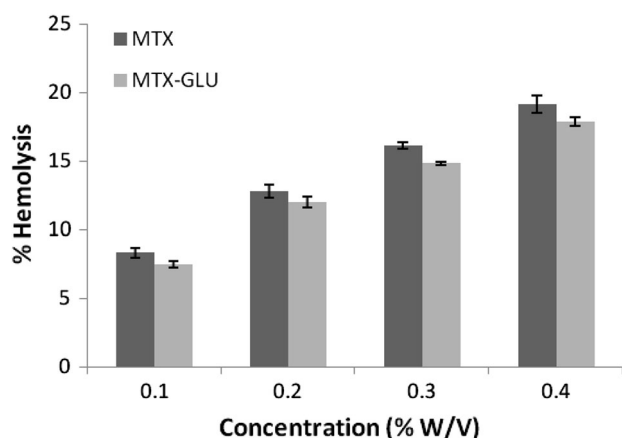
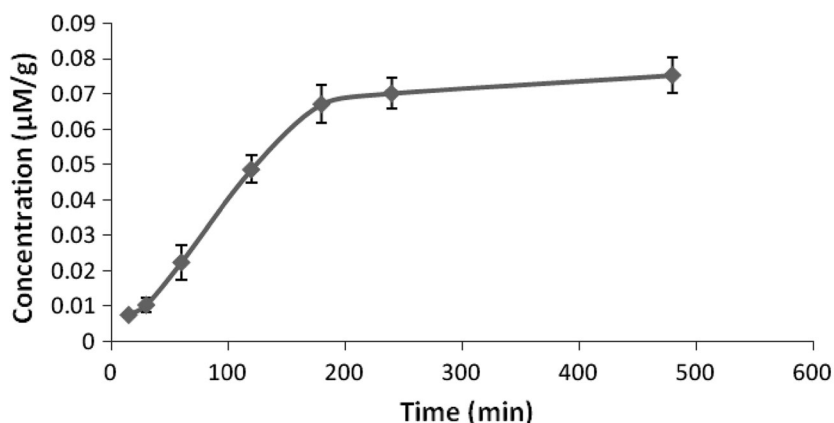
MTX–GLU	Kinetic constant	
	$K$ ( $\text{min}^{-1}$ )	$t_{1/2}$ (min)
Plasma	$3.11 \times 10^{-3}$	$229.17 \pm 6.37$
Brain homogenate	$5.38 \times 10^{-3}$	$128.70 \pm 1.27$

$n = 3$

**Table 3** In vitro log *D* and binding of MTX–GLU to plasma protein

Compound	log <i>D</i>	Plasma protein binding (%)			
		10 (µg/ml)	20 (µg/ml)	50 (µg/ml)	100 (µg/ml)
MTX–GLU	–1.78	40.26 ± 3.0	41.39 ± 0.84	35.42 ± 0.28	43.41 ± 2.64
MTX	–1.85	43.54 ± 1.56	38.93 ± 3.23	40.54 ± 2.16	40.72 ± 1.18

*n* = 3

**Fig. 1** Release of the MTX by MTX–GLU in brain homogenate (mean ± SD, *n* = 3)**Fig. 2** Percent haemolysis with MTX and MTX–GLU (mean ± SD, *n* = 3)

studies in vitro demonstrated favourable features, we proceeded with the in vivo studies.

#### Toxicity study

The MTX–GLU was well tolerated as suggested by the toxicity studies done as per the guidelines of Organization of Economic Co-operation and Development (OECD-423) for testing of chemicals (Regd. No.-1283/c/09/CPCSEA). The haemolytic toxicity of MTX is a major limitation for its use. Thus haemolytic toxicity was measured in terms of

percent RBC haemolysis to monitor toxicity of MTX–GLU. It exhibited relatively less haemolytic toxicity (Fig. 2).

Further to determine safety of the prodrug, haematological parameters were determined to study its effect on different components of blood. Blood samples were analysed for RBC count, WBC count, haematocrit (HCT), haemoglobin (Hb) and differential lymphocytes count at a pathology laboratory (Table 4). This suggests that MTX–GLU has not been able to mask the toxic profile of MTX, at the same time it has also not made it more toxic. Accordingly, for in vivo studies, the dose profiles can be considered similar to that of MTX.

#### In vivo release of MTX

To understand the in vivo behaviour of conjugate, we assessed the plasma pharmacokinetics of MTX and MTX–GLU. Pharmacokinetic parameters in blood are reported (Table 5). Free MTX from MTX–GLU and MTX presented with an area under the concentration–time profile ( $AUC_{0-t}$ ) exhibited an increment of 54.05 % compared to the parent drug. This indicated relatively prolonged plasma maintenance of MTX–GLU. The mean residence time (MRT) of MTX after administration of the MTX–GLU increased by 40.63 %. The half life of MTX from MTX–GLU was 23.86 % more than the parent drug. This suggested that it has helped to increase its circulation time in plasma which may help the process of transportation across

**Table 4** Haematological parameters of animals treated with MTX and MTX–GLU after 15 days

Formulations	Dose (mg/kg)	RBC count ( $\times 10^6/\mu\text{l}$ )	WBC count ( $\times 10^3/\mu\text{l}$ )	Differential count ( $\times 10^3/\mu\text{l}$ )			Hb (g/dl)	HCT
				Monocytes	Lymphocytes	Neutrophils		
Control	Nil	9.2 $\pm$ 0.2	10.9 $\pm$ 0.2	1.0 $\pm$ 0.1	8.8 $\pm$ 0.2	1.84 $\pm$ 0.1	12.5 $\pm$ 0.2	38.43 $\pm$ 1.5
MTX	25	8.2 $\pm$ 0.4	13.2 $\pm$ 0.4	0.92 $\pm$ 0.1	9.4 $\pm$ 0.3	2.28 $\pm$ 0.1	10.5 $\pm$ 0.4	32.74 $\pm$ 2.3
	250	7.4 $\pm$ 0.1	15.4 $\pm$ 0.6	0.8 $\pm$ 0.07	10.0 $\pm$ 0.6	3.02 $\pm$ 0.3	9.4 $\pm$ 0.5	29.37 $\pm$ 0.8
MTX–GLU	25	8.4 $\pm$ 0.2	12.8 $\pm$ 0.3	0.9 $\pm$ 0.1	9.5 $\pm$ 0.3	2.17 $\pm$ 0.1	10.6 $\pm$ 0.2	33.22 $\pm$ 2.8
	250	7.2 $\pm$ 0.2	14.8 $\pm$ 0.4	0.8 $\pm$ 0.07	10.6 $\pm$ 0.3	2.90 $\pm$ 0.2	9.6 $\pm$ 0.5	30.03 $\pm$ 0.7

$n = 6$ . Albino rats per group, all the tabulated values represent mean  $\pm$  SD RBC, WBC, Hb and HCT represent red blood corpuscles, white blood corpuscles, haemoglobin and haematocrit, respectively

**Table 5** Pharmacokinetic parameter of MTX in Plasma after administration of MTX and MTX–GLU

Compound	AUC <sub>0–t</sub> ( $\mu\text{M}/\text{ml min}$ )	AUMC <sub>0–t</sub> ( $\mu\text{M}/\text{ml min}^2$ )	MRT (min)	$t_{1/2}$ (min)
MTX	15.65 $\pm$ 0.61	1093.41 $\pm$ 84.04	69.77 $\pm$ 2.58	48.61 $\pm$ 1.89
MTX–GLU	24.11 $\pm$ 0.52****	2367.06 $\pm$ 101.14****	98.12 $\pm$ 2.64****	60.21 $\pm$ 3.70**

$n = 3$ . \*\*  $P < 0.001$  with respect to MTX, \*\*\*  $P < 0.001$  with respect to MTX, \*\*\*\*  $P < 0.0001$  with respect to MTX

**Table 6** Pharmacokinetic parameter of MTX in brain after administration of MTX and MTX–GLU

Compound	AUC <sub>0–t</sub> ( $\mu\text{M}/\text{g min}$ )	AUMC <sub>0–t</sub> ( $\mu\text{M}/\text{g min}^2$ )	MRT (min)	$C_{\text{max}}$ ( $\mu\text{M}/\text{g}$ )	$T_{\text{max}}$	REs	CEs
MTX	1.21 $\pm$ 0.05	69.97 $\pm$ 3.12	57.29 $\pm$ 1.00	0.014	30	–	–
MTX–GLU	6.98 $\pm$ 0.13****	626.60 $\pm$ 65.24 ****	89.54 $\pm$ 7.83***	0.074****	30	5.76	5.28

$n = 3$ . \*\*\*\*  $P < 0.0001$  with respect to MTX, \*\*\*  $P < 0.001$  with respect to MTX

BBB. To further evaluate the possible transport of MTX–GLU across BBB, distribution of MTX to brain from i.v. administration was studied (Table 6). The AUC<sub>0–t</sub> and  $C_{\text{max}}$  of MTX in brain after i.v. administration of MTX–GLU were significantly higher than that after the injection of naked MTX. The relative uptake efficiency (RE) was 5.76 times for the MTX–GLU. The concentration efficiency (CE) was 5.28 times. These results indicated that MTX–GLU delivered MTX across BBB successfully (Fig. 3).

#### Relative tissue distribution of MTX–GLU to brain and other tissues

The radio labelling of MTX and MTX–GLU was done following established method using  $^{99\text{m}}\text{Tc}$  (Reddy *et al.*, 2004; Vyas *et al.*, 2006). The amount of  $\text{SnCl}_2 \cdot 2\text{H}_2\text{O}$ , and incubation time for radio labelling were optimised (Table 7). MTX–GLU labelled with  $^{99\text{m}}\text{Tc}$  exhibited more than 96 % radio labelling efficiency. The radiochemical impurity that is likely to exist in the form of unconjugated technetium was found to be 2.85 % of MTX–GLU. The labelled conjugates were found to be stable in normal saline solution and in mice plasma up to 4 h (degradation

$< 5$  % w/w) (Table 8). Thus, these formulations were found to be suitable for conducting radiosciography studies in mice.

The stable radiolabelled MTX and MTX–GLU were used for biodistribution study. It was injected (equivalent to 2.80  $\mu\text{M}/\text{kg}$  body weight) through the tail vein of Swiss albino mice. Radioactivity present in each tissue/organ was measured using shielded well-type gamma scintillation counter as % radioactivity. Measurement and expression of exact biodistribution to tissues are subject to many limitations. Thus, tissue to blood ratio is an important parameter to indicate drug distribution (Poulin and Theil 2000; Muller *et al.*, 2004). Accordingly, blood label after 15 min of administration was considered 100 % and relative distribution to other tissues expressed as percentage of it (Table 9).

Considering the fact that MTX level in brain from both MTX and MTX–GLU reached the highest level during 60 min of administration (Fig. 3) and stability of radiolabelled compound (4 h), distribution data were compiled up to 120 min of administration. Both were widely distributed to tissues including liver, spleen, lung and kidney as observed from radiosciography images (Fig. 4) and radio activity count (Table 9). The drug level reduced with time

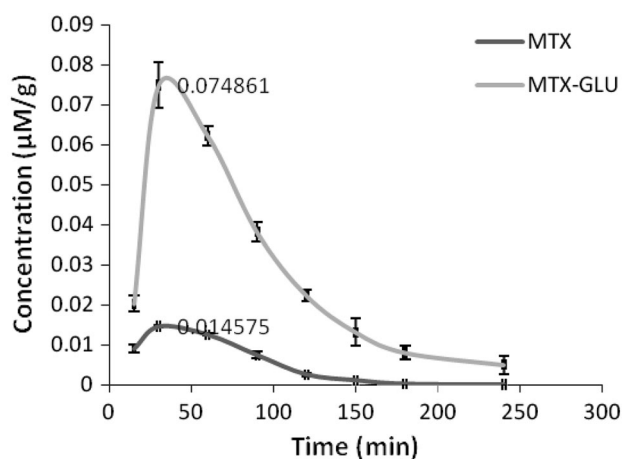


**Fig. 3** Concentration of MTX in brain after administration of MTX and MTX-GLU

suggesting tissue up take and elimination. Distribution to heart tissue was less and comparable for both MTX-GLU and the parent drug. The liver and spleen level of MTX and MTX-GLU increased up to 30 min and then decreased with time. Distribution of both parent drug and MTX-GLU was similar to stomach and intestine with respect to time. Relatively low distribution of MTX-GLU to lung tissue suggests less fast-pass lung elimination of the MTX-GLU. In contrast to this, higher distribution to kidney suggests significance of its elimination by this route. However, distribution to brain tissue presents a very contrast figure. The brain level of MTX-GLU was 9.07 % by 15 min and increased up to 39.92 % of initial plasma level by 30 min and then decreased gradually. The ratio of brain to blood level was 36.33 % (Fig. 4). This indicates effective transport of MTX-GLU across BBB. The polar nature of MTX-GLU cannot justify its higher brain penetration. Amino acids analogues have earlier been found to penetrate BBB facilitated by amino acid carrier system (Greig *et al.*, 1987). Accordingly, the significant brain permeability suggests involvement of a similar kind of system. Further investigations are necessary to elucidate its mode of interaction with specific transportation system. Since these amino acid transporters are also expressed in tumours, MTX-GLU may have potential for higher uptake (Begleiter *et al.*, 1979; Goldenberg *et al.*, 1979; Samnick *et al.*,

**Table 8** In vitro stability of radiolabelled complexes of MTX and MTX-GLU

Time (h)	Radio labelling efficiency (%)			
	MTX		MTX-GLU	
	Saline	Plasma	Saline	Plasma
1	94.2 ± 0.3	94.0 ± 0.7	96.8 ± 0.5	95.6 ± 0.5
2	93.3 ± 0.4	92.7 ± 0.8	95.2 ± 0.7	94.8 ± 0.4
4	91.6 ± 1.0	90.1 ± 0.9	94.0 ± 0.4	93.6 ± 0.6

$n = 3$

2004; Wang *et al.*, 2011). Further studies are being carried out to explore this as well as to evaluate its safety profile in order to establish its suitability as a prodrug.

## Experimental

### Chemistry

All the reactions were performed with reagents of commercial high purity without further purification. Reactions were monitored by thin-layer chromatography. Purifications of the compounds were performed by crystallisation and column chromatography. Purity of the final compound was determined to be >95 % by an analytical HPLC (Yunglin Liquid Instrument, Korea) on a promocil C18 column (4.6 mm × 250 mm, 5 µm). FTIR spectra were recorded in KBr discs on IR solution Version Affinity 1 (Shimadzu, Japan); the data were in agreement with the structure of the compounds. <sup>1</sup>H and <sup>13</sup>C NMR spectra were recorded on a Bruker Avance II 400 spectrometer (Bruker Biospin, Fällanden, Switzerland) operating at 400.136 MHz and 100.61, respectively, using tetramethylsilane as an internal standard. The final product was also characterised by mass spectroscopy with Q-ToF micromass spectrometer (Waters, Milford Massachusetts, USA) equipped with an electrospray ionization source. Elemental analysis was carried out on a 2,400 series II CHNS/O analyser, Perkin Elmer, USA. Yunglin liquid chromatography system equipped with a isocratic pump, dual wavelength UV/VIS absorbance detector (UV730D) and manual sample injector with switch (7725i) was used (YL

**Table 7** Radiolabelling of MTX and MTX-GLU

Formulation	Incubation time (min)	Conc. of SnCl <sub>2</sub> (µg)	pH	Labelling efficiency (%)	Reduced/hydrolysed (%)	Free <sup>99m</sup> Tc-(%)
MTX	15	120	7.3	94.2 ± 0.3	0.6 ± 0.02	5.2 ± 0.2
MTX-GLU	20	80	6.5	96.8 ± 0.5	0.35 ± 0.03	2.85 ± 0.5

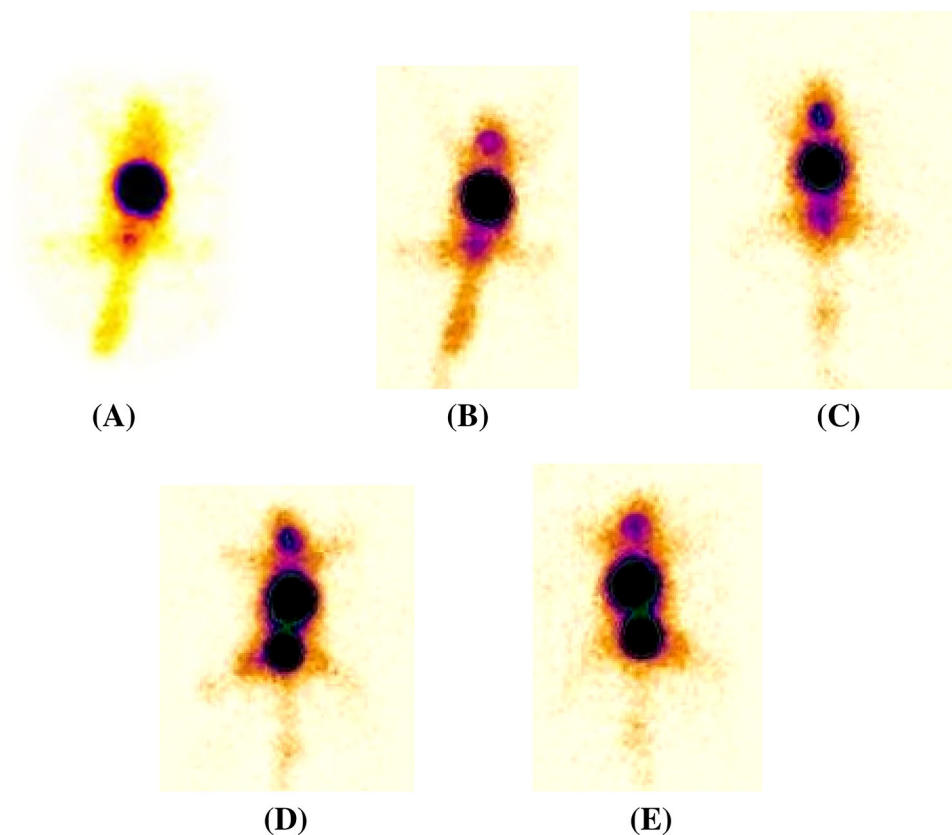
$n = 3$

**Table 9** Relative tissue distribution (%) of MTX and MTX–GLU

Organ	Time interval (min)							
	15		30		60		120	
	MTX	MTX–GLU	MTX	MTX–GLU	MTX	MTX–GLU	MTX	MTX–GLU
Blood	100	100	90.37	115.69	83.95	73.23	46.52	62.46
Heart	42.24	43.76	44.38	27.53	30.48	25.23	26.73	20.46
Lung	229.99	222.38	282.35	85.53	75.40	77.53	50.80	61.07
Liver	1,206.95	1,283.07	1,580.21	1,026	1,252.40	872.76	1,181.81	809.69
Spleen	255.0	311.23	347.59	295.69	286.09	232.15	127.27	277.23
Kidney	179.14	209.38	135.82	252.30	174.33	159.38	166.84	139.16
Stomach	27.27	26.76	22.99	20.76	20.85	20	20.32	14.61
Intestine	39.57	25.84	28.87	20.30	26.73	19.69	12.29	17.07
Brain	3.2	9.07	1.6	39.92	1.6	26.61	1.06	16.76

Plasma level of MTX and MTX–GLU at 15 min is considered 100 %

**Fig. 4** Gamma scintigraphy images of mice for **a** MTX after 120 min and that of MTX–GLU after **b** 15 min, **c** 30 min, **d** 60 min **e** 120 min



Instrument, Korea) for HPLC analysis.  $^{99m}\text{Tc}$ -pertechnetate was provided by INMAS, Delhi, India. The radioactivity counter was a gamma ray counter (Type GRS23C, serial no. 458-425 Electronic Corporation of India Limited, India). Imaging of animal was performed using Single

Photon Emission Computerized Tomography (SPECT, LC 75-005, Diacam, Siemens AG, Erlanger, Germany) gamma camera. Animal Handling and experimentation were carried out as per the guideline of the Institutional Animal Ethical Committee.

*Procedure for 2-(4-(((2,4-bis(2-amino-4-carboxybutanamido)pteridin-6-yl)methyl)(methyl) amino) benzamido) pentanedioic acid (3)*

Glutamic acid (20 mmol) was added to a stirred solution of NaOH (25 mmol) in 50 ml of water at ambient temperature and then diluted with 50 ml of 1,4-Dioxane and Di-*tert*-butyl dicarbonate (20 mmol) was added drop wise. The reaction was brought to completion by further stirring for 16 h at room temperature. The solution was concentrated under reduced pressure. This mixture was cooled in an ice bath and covered with a layer of diethyl ether (10 ml). The reaction mixture was extracted with (20 ml × 2) of diethyl ether, and the organic phase extracted with (30 ml × 3) of saturated aqueous sodium bicarbonate solution. The combined aqueous layer was acidified to pH 2 by addition of potassium hydrogen sulphate solution. The mixture was extracted with (30 ml × 2) of ethyl ether. The organic layer was dried over MgSO<sub>4</sub>, filtered and evaporated under rotary evaporator. Hexane was added to the thick oil to turbidity. The mixture is allowed to stand for 1 h. The white crystalline solid was collected by filtration, washed with (10 ml × 3) portions of hexane and dried under reduced pressure to get 2-((*tert*-butoxycarbonyl)amino)pentanedioic acid (**1**) with yield of 4.25 g (85 %).

Methotrexate (2 mmol) was taken in 50 ml of dry dichloromethane and 4-dimethylaminopyridine (1.6 mmol) was added to it. The mixture was stirred and cooled in an ice bath to 0 °C. Compound **1** (6 mmol) was taken in dichloromethane (10 ml) and 2.2 mmol of dicyclohexylcarbodiimide (DCC) in dichloromethane was added over a 5-min period. The pH (3) was monitored during this. This mixture was stirred at 0 °C for 2 h and added to the ice-cooled reaction mixture of MTX drop wise with stirring. The resulting reaction mixture was stirred for 24 h at room temperature. The precipitate was removed by filtration and the filtrate was concentrated under vacuum and taken up in ethyl acetate and washed with 5 % of aqueous acetic acid solution (3 × 20 ml) and 1 M sodium carbonate (3 × 20 ml). This washed organic solution was dried over anhydrous sodium sulphate and concentrated in vacuum. A viscous yellow crude product was obtained. This was recrystallised. Further purification of crude product was done by column chromatography using dichloromethane: acetonitrile: methanol (1:1:2) as mobile phase. The major fraction was separated and recrystallised to afford 2-(4-(((2,4-bis(2-(*tert*-butoxycarbonylamino)-4-carboxybutanamido)pteridin-6-yl)methyl)(methyl)amino)benzamido)pentanedioic acid (**2**) in 53 % yield.

To this compound **2** (1 mmol) trifluoroacetic acid (TFA, 4.5 ml) was added drop wise in 5 ml dichloromethane at 0 °C in an ice bath. The reaction was left to stir for 1.5 h,

then the reaction was saturated with diethyl ether until precipitate formed. The precipitate was decanted off, washed twice with diethyl ether then dried over anhydrous sodium sulphate and evaporated under vacuum to obtain the desired product as a dry light brownish solid. It was triturated in ethyl acetate (10 ml) and purified in column chromatography using dichloromethane: methanol: water (1:2:1) as mobile phase. Following recrystallisation, the compound **3** was recovered.

*2-(4-(((2, 4-bis (2-amino-4-carboxybutanamido) pteridin-6-yl) methyl) (methyl) amino) benzamido) pentanedioic acid (3)* Yellow solid. Yield: 70 %. m.p.: 205–208 °C. Analysis for C<sub>30</sub>H<sub>36</sub>N<sub>10</sub>O<sub>11</sub> (712.257); calculated: C, 50.56; H, 5.09; N, 19.65; found: C, 50.66; H, 5.07; N, 19.70. FTIR (KBr),  $\nu(\text{cm}^{-1})$ : 3964.45 (O–H), 3306.03 (N–H), 3198.03 (N–H), 1705.07 (C=O), 1683.86 (CONH), 1517.05 (C=N). <sup>1</sup>H NMR(DMSO)  $\delta$  (ppm): 11.28 (s, 1H, OH), 11.18 (s, 1H, OH), 11.05 (s, 1H, OH), 8.55 (s, 2H, NH<sub>2</sub>), 8.31 (s, 1H, NH), 8.31 (s, 1H, NH), 8.30 (s, 1H, NH), 8.16 (s, 1H, NH), 8.15 (s, 1H, Pyrazine), 6.59–7.80 (m, Ar–H), 4.78 (s, 2H, CH<sub>2</sub>), 4.37–4.41 (m, 1H, CH), 3.38 (s, 3H, CH<sub>3</sub>), 4.78 (s, 2H, CH<sub>2</sub>), 3.22–3.40 (t, 1H, CH), 2.52–2.54 (m, 2H, CH<sub>2</sub>), 2.32–2.36 (t, 2H, CH<sub>2</sub>), 2.10–2.14 (m, 2H, CH<sub>2</sub>), 2.05–2.09 (t, 2H, CH<sub>2</sub>). <sup>13</sup>C NMR (DMSO)  $\delta$  (ppm): 174.15 (COOH), 173.87 (COOH), 172.48 (COOH), 171.25 (CONH), 170.14 (CONH), 166.25 (CONH), 162.64 (CN, Pyrimidine), 162.48 (CN, Pyrimidine), 154.68 (CN, Pyrazine), 150.84 (CN, Pyrazine), 148.83 (Pyrazine), 146.00 (Pyrazine), 128.78 (2C, 1-benzene), 121.49 (Benzene), 121.34 (Benzene), 11.91 (2C, 1-benzene), 55.48 (CNH<sub>2</sub>), 53.87 (CNH<sub>2</sub>), 52.94 (CNH), 52.01 (CN), 39.99 (CH<sub>3</sub>N), 33.68 (CH<sub>2</sub>), 33.05 (CH<sub>2</sub>), 31.57 (CH<sub>2</sub>), 30.59 (CH<sub>2</sub>), 30.15 (CH<sub>2</sub>), 27.59 (CH<sub>2</sub>), MS *m/z* (%): 713.32 (M+1).

#### Stability studies in different buffer solutions

The MTX–GLU was investigated for their chemical stability in phosphate buffer solution at four pH values: 2.0, 4.9, 7.4 and 8.0 at 37 °C. Precisely, 1 ml methanol solution (0.140  $\mu\text{M}/\text{ml}$ ) of the prodrug was added into 4 ml of different buffers at 37 °C. After mixing, it was kept in a 37 ± 1 °C constant water bath and then 200  $\mu\text{l}$  samples were withdrawn at different time points (0, 1, 2, 4, 8, 12 and 24 h). The disappearance of MTX–GLU was monitored by HPLC method. The rate constant ( $K_{\text{disapp}}$ ) and half lives ( $t_{1/2}$ ) of the compounds in aqueous solution were calculated by linear regression of peak area against time.

#### Stability in plasma extracts and brain homogenate

Blood was drawn from mice through orbital sinus and was collected in a heparinised tube paved with heparin sodium.



Samples were centrifuged at 15,000 rpm for 15 min to separate plasma which was diluted with double volumes of water. The brain was removed and homogenised in cold phosphate buffer of pH 7.4 with proportion of 1:5 (w/v). Samples were then placed on ice and used immediately. 1 ml sol of MTX–GLU (0.140  $\mu\text{M}/\text{ml}$ ) in PBS 7.4 was added to plasma and brain homogenate, respectively, and gently vortexed. Samples were incubated at 37 °C and 200  $\mu\text{l}$  aliquots were removed after 15, 30, 60, 90 and 120 min, respectively. Following deproteinisation and centrifugation, the supernatants were analysed by HPLC.

#### Conversion of MTX–GLU to MTX in brain homogenate

Brain was removed and homogenised in cold phosphate buffer of pH 7.4 with proportion of 1:5 (w/v). Samples were then placed on ice and used immediately. 1 ml sol of MTX–GLU (0.140  $\mu\text{M}/\text{ml}$ ) in PBS 7.4 was added to brain homogenate and gently vortexed. The pH was adjusted to acidic with 10 % phosphoric acid. Samples were incubated at 37 °C and 200  $\mu\text{l}$  aliquots were removed after 15, 30, 60, 120, 180, 240 and 480 min, respectively. Samples were deproteinised, centrifuged and the supernatants were analysed by HPLC for determination of MTX. The mobile phase was composed of phosphate buffer (10 mmol dihydrogen phosphate and 10 mmol sodium hydroxide, pH 7.4) premixed, filtered and degassed buffer in water: acetonitrile (90:10) at a flow rate of 1 ml/min. The retention time of MTX was found to be at 7.3 min. The UV detector was set to monitor the signal at 310 nm corresponding to the maximum absorbance for MTX.

#### Distribution coefficients of MTX–GLU

The 1-octanol/water distribution coefficient ( $\log D$ ) was determined by shake flask method. The compound was dissolved in PBS 7.4 to a concentration of 1.40  $\mu\text{M}/\text{ml}$ . The solution was carefully diluted with PBS 7.4, to obtain a series of known concentrations in order to create a calibration curve. Using aqueous (PBS) solutions of MTX–GLU (1.40  $\mu\text{M}/\text{ml}$ ), stock solutions were prepared with corresponding volumes of 1-octanol (the ratio varied with the compounds). The mixture was kept for 24 h on a mechanical shaker and then allowed to stand long enough to separate the phases and achieve a saturation state. Concentration in the aqueous phase was determined by using UV–Visible spectrophotometer. Based on a simple mass balance, concentration in the octanol phase was determined and the  $\log D$  was calculated as the ratio of the concentration in the octanol phase to the concentration in the aqueous phase.

#### Protein binding study

Protein binding study was done following reported procedure (Rajput *et al.*, 2012). Blood from goat was collected, heparinised and kept in deep freezer at  $-20$  °C. Plasma was separated with aid of cooling centrifuge at 6,000 rpm. Various concentrations of MTX and MTX–GLU (10, 20, 50 and 100  $\mu\text{g}/\text{ml}$ ) were prepared in plasma. Each dialysing bag filled with 5 ml of plasma, containing a known amount of the drug, was then immersed in flask containing 5 ml of phosphate buffer 7.4 and the flasks were incubated at 37 °C for 24 h with orbital shaker at 50 rpm. At the end of the incubation period, the buffer as well as the contents of the dialysing bags was analysed separately by UV spectrophotometer and plasma protein binding was calculated.

#### In vitro haemolytic toxicity study

Toxicity studies were carried out as per the guidelines of Organization of Economic Co-operation and Development (OECD-423) for testing of chemicals (Regd. No.-1283/c/09/CPCSEA). The degree of haemolysis was determined as per the reported method (Singhai *et al.*, 1997). The RBCs were separated from the whole blood by centrifugation (REMI, Mumbai, India) at 3,000 rpm for 5 min. The supernatants and buffy coats were removed and discarded. The packed cell volume (PCV) was washed with normal saline and centrifuged again at 2,000 rpm for 2 min. The 5 ml of PCV was then diluted to 100 ml with normal saline to get 5 % RBC suspension. 0.5 ml of suitably diluted (0.1, 0.2, 0.3 and 0.4 %) plain MTX and MTX–GLU was added to 4.5 ml of normal saline and incubated for 1 h with RBC suspension. After centrifugation, supernatants were taken and diluted with an equal volume of normal saline and absorbance was measured at 540 nm. RBC suspension was added to 5 ml of saline and 5 ml distilled water, respectively, to obtain 0 and 100 % haemolysis.

#### In vivo haematological studies

Healthy male albino rats of Sprague–Dawley strain of uniform body weight ( $200 \pm 10$  g) were selected for the study of haematological parameters. Fifteen animals were selected and divided into three groups comprised three rats in each group. 25 and 250 mg/kg body weight of MTX and MTX–GLU were separately administered, intravenously into second and third groups of animals, respectively, daily up to 7 days. The first group was kept as control, which was maintained on same regular diet for 7 days. After 15 days, blood samples were collected from the animals of all the groups and analysed for RBC count, WBC count, haematocrit (HCT), haemoglobin content, differential

monocyte count, lymphocytes and neutrophils by pathology laboratory.

#### In vivo release of MTX from MTX–GLU

Mice were randomly divided into 2 groups, 24 in each group for different sampling times and housed in one cage. Each animal was injected with MTX or MTX–GLU in phosphate buffer of pH 7.4 through the tail vein at a single dose equivalent to 7.2  $\mu\text{M}/\text{kg}$  body weight of MTX. At appropriate time interval (15, 30, 60, 90, 120, 150, 180 and 240 min), the animal was sacrificed and 1 ml blood samples withdrawn from cardiac puncture were collected in heparinized tube. Plasma was immediately separated by centrifugation and diluted with PBS 7.4–1:3 which was stored at  $-20\text{ }^\circ\text{C}$  until assay. Meanwhile, the brain sample was removed and weighed. Each tissue sample was homogenised and diluted with PBS 7.4–1:3 (g/ml). The homogenates were also stored at  $-20\text{ }^\circ\text{C}$  until assay. Before analysing conjugate, hydrolysis was performed. After deproteinization, the mixture was centrifuged at 15,000 rpm for 15 min. 200  $\mu\text{l}$  aliquots were withdrawn, and 200  $\mu\text{l}$  of acetonitrile was added to each aliquot and vortexed. Samples were centrifuged for further 15 min to remove residual proteins and the supernatants were analysed by HPLC method.

#### Radio labelling of MTX and MTX–GLU with $^{99\text{m}}\text{Tc}$ and optimisation

$^{99\text{m}}\text{Tc}$ -pertechnetate was provided by INMAS, Delhi, India. The radioactivity count was done with a gamma ray counter (Type GRS23C, serial no. 458-425 Electronic Corporation of India Limited, India). Imaging of animal was performed using Single Photon Emission Computerized Tomography (SPECT, LC 75-005, Diacam, Siemens AG, Erlanger, Germany) gamma camera. Animal Handling and experimentation were carried out as per the guideline of the Institutional Animal Ethical Committee.

The radiolabelling of MTX and MTX–GLU conjugates was done by dissolving the 2.0 mg equivalent of drug in 1 ml water for injection in a sterile glass vial. Then, followed by addition of stannous chloride, pH was adjusted at 7.0 using 0.5 M sodium bicarbonate solution. To the resulting mixture (filtered through 0.22  $\mu\text{m}$  membrane filter), 1–2 ml of 74 MBq  $^{99\text{m}}\text{Tc}$ -pertechnetate containing 2.0–3.0 mCi was added drop wise and the reaction mixture was incubated at  $25 \pm 5\text{ }^\circ\text{C}$  for 15–20 min and checked for radiolabelling efficiency by thin-layer chromatography method (Reddy *et al.*, 2004). The procedure involved spotting 2  $\mu\text{l}$  samples of radiopharmaceuticals onto chromatographic strip 10 cm in length. After developing in the solvent, the strip was cut into two portions (top:bottom:

1:3) and activity in each portion was measured in the form of count using gamma scintillation counter.  $^{99\text{m}}\text{Tc}$ -labelled MTX and  $^{99\text{m}}\text{Tc}$ -labelled MTX–GLU remained at the origin and free technetium travelled with the solvent front. The radiolabelling yield was expressed as a percentage of the total amount of radioactivity applied in the testing system. The radiolabelling efficiency was calculated using established equation (Babbar *et al.*, 2000). Radiochemical impurity that is likely to exist in the form of unconjugated technetium in  $^{99\text{m}}\text{Tc}$ -labelled MTX–GLU conjugates and  $^{99\text{m}}\text{Tc}$ -labelled MTX solution was determined by the instant thin-layer chromatography–silica gel (ITLC–SG) strips as stationary phase. The effects of incubation time, pH and stannous chloride concentration on labelling were studied to achieve optimum reaction conditions (Table 7). The in vitro stability of radiolabelled formulation was evaluated in 0.9 % (w/v) sodium chloride and in mice plasma. After the optimisation and evaluation, stable radiolabelled MTX and MTX–GLU were used for biodistribution study in mice.

#### Biodistribution study and radioscintigraphy imaging in mice

Swiss albino mice (2–3-month old of either sex) weighing 22–30 g of BALB/c strain were used for biodistribution studies. Animals were procured from the National center of disease control, Sham Nath Marg, Delhi, India. The animals were selected at random from the stock colony maintained in the animal house facility. The animals were reared on laboratory chow pellets, fed ad libitum and had free access to food and water at all the time. The room was maintained at  $25 \pm 2\text{ }^\circ\text{C}$  with natural daytime light and no light after 12 h until morning.

Three mice for each drug and prodrug per time point (15, 30, 60 and 120 min) were used in the study. 3.7 MBq of radiolabelled compound containing 2 mg of MTX and MTX–GLU (equivalent to 2.80  $\mu\text{M}/\text{kg}$  body weight) was injected through the tail vein of each mouse. The mice were killed humanely at different time intervals and the blood was collected using cardiac puncture. Subsequently, brain, lungs, heart, liver, kidney, spleen, intestine and stomach were dissected, washed twice using normal saline, made free from adhering tissue/fluid and weighed. Radioactivity present in each tissue/organ was counted using shielded well-type gamma scintillation counter and expressed as % of radioactivity in blood to tissue relative distribution.

Gamma scintigraphy imaging was performed on mice following i.v. administrations of radiolabelled drug and its prodrug to determine the localisation of drug in brain. 18.5 MBq of radiolabelled compound containing 2 mg of MTX and MTX–GLU (equivalent to 2.80  $\mu\text{M}/\text{kg}$  body

weight) was injected through the tail vein of each mouse. The mice were anaesthetized using 0.4 ml ketamine (50 mg/ml) intramuscular injection and placed on the imaging board. Imaging was performed using gamma scintillation camera.

### Statistical analysis

All experiments were conducted at least in triplicate and results were expressed as mean  $\pm$  SD. The  $AUC_{0-t}$ ,  $AUMC_{0-t}$  and MRT were calculated by nonlinear Trapezoidal rule. Statistical evaluation (Graphpad prism 5.0 demo version) was performed by unpaired *t* test with 95 % confidence interval.  $P < 0.001$  was considered significant. The RE and CE were calculated to evaluate the brain targeting property of prodrug. The value of RE and CE was defined as following:

REs (relative uptake efficiencies)

$$= (AUC_{0-t})_{\text{sample}} / (AUC_{0-t})_{\text{control}}$$

CEs (concentration efficiencies)

$$= (C_{\text{max}})_{\text{sample}} / (C_{\text{max}})_{\text{control}}$$

**Acknowledgments** The authors are thankful to Dr. Anil Kumar Mishra, HOD and Joint Director, Division of Cyclotron and Radiopharmaceutical Sciences, Institute of Nuclear Medicine and Allied Sciences (INMAS), Delhi for his permission and Dr. Krushna Chuttani, Scientist, INMAS for her help in carrying out radioscintigraphy experiments. We are also thankful to Sophisticated Analytical Instrumentation Facility, Panjab University, Chandigarh for help in spectral characterisation and IPCA laboratories, Daman, India for providing methotrexate as gift sample.

### References

- Al-Sarraf H, Preston JE, Segal MB (1995) The entry of acidic amino acids into brain and CSF during development, using in situ perfusion in the rat. *Dev Brain Res* 90:151–158
- Al-Sarraf H, Preston JE, Segal MB (1997a) Changes in the kinetics of the acidic amino acid brain and CSF uptake during development in the rat. *Dev Brain Res* 102:127–134
- Al-Sarraf H, Preston JE, Segal MB (1997b) Acidic amino acid accumulation by rat choroid plexus during development. *Dev Brain Res* 102:47–52
- Babbar AK, Singh K, Goel HC (2000) Evaluation of  $^{99m}\text{Tc}$  labeled Photosan-3, a heamatorporphyrin derivative, as a potential radiopharmaceutical for tumor scintigraphy. *Nucl Med Biol* 27:419–426
- Batchelor T, Carson K, O'Neill A (2003) Treatment of primary CNS lymphoma with methotrexate and deferred radiotherapy: a report of NABTT 96–07. *J Clin Oncol* 21:1044–1049
- Bauwens M, Lahoutte T, Kersemans K (2007) D- and L-[ $^{123}\text{I}$ ]-2-I-phenylalanine show a long tumour retention compared with D- and L-[ $^{123}\text{I}$ ]-2-I-tyrosine in R1M rhabdomyosarcoma tumour-bearing Wag/Rij rats. *Contrast Media Mol Imaging* 2:172–177
- Begleiter A, Lam H, Grover J (1979) Evidence for active transport of melphalan by amino acid carriers in L5178Y lymphoblasts in vitro. *Cancer Res* 39:353–359
- Combe B, Edno L, Lafforgue P (1995) Total and free methotrexate pharmacokinetics, with and without piroxicam, in rheumatoid arthritis patients. *Rheumatology* 34:421–428
- Czerebys M, Mysiorek C, Kulikova N, Samluk L, Berezowski V, Cecchelli R, Nale KA (2008) A polarized localization of amino acid/carnitine transporter  $B^{0,+}$  ( $ATB^{0,+}$ ) in the blood–brain barrier. *Biochem Biophys Res Commun* 376:267–270
- De Angelis LM, Seiferheld W, Schold SC (2002) Combination chemotherapy and radiotherapy for primary central nervous system lymphoma: radiation therapy oncology group study 93–10. *J Clin Oncol* 20:4643–4648
- Donehower RC, Hande KR, Drake JC (1979) Presence of 2,4-diamino-N10-methylptericoic acid after high-dose methotrexate. *Clin Pharmacol Ther* 26:63–72
- Drewes LR, Conway WP, Gilboe DD (1977) Net amino acid transport between plasma and erythrocytes and perfused dog brain. *Am J Physiol* 233:320–325
- Ennis SR, Kawai N, Ren XD, Abdelkarim GE, Keep RF (1998) Glutamine uptake at the blood–brain barrier is mediated by N-system transport. *J Neurochem* 71(6):2565–2573
- Erdlenbruch B, Schinkhof C, Kugler W (2003) Intracarotid administration of short-chain alkylglycerols for increased delivery of methotrexate to the rat brain. *Br J Pharmacol* 139:685–694
- Gabathuler R (2010) Approaches to transport therapeutic drugs across the blood–brain barrier to treat brain diseases. *Neurobiol Dis* 37:48–57
- Geiera EG, Schlessingera A, Fana H, Gable JE, Irwina JJ, Salia A, Giacomina KM (2013) Structure-based ligand discovery for the large-neutral amino acid transporter 1, LAT-1. *PNAS* 110(14):5480–5485
- Goldenberg G, Lam H, Begleiter A (1979) Active carrier-mediated transport of melphalan by two separate amino acid transport systems in LPC-1 plasmacytoma cells in vitro. *J Biol Chem* 254:1057–1064
- Gourav K, Goel RK, Shukla M, Pandey M (2012) Glutamine as a neuroprotective agent in high-dose paclitaxel-induced peripheral neuropathy: a clinical and electrophysiologic study. *Indian J Med Paediatr Oncol* 33(1):13–20
- Greig NH, Momma S, Sweeney DJ (1987) Facilitated transport of melphalan at the rat blood–brain barrier by the large neutral amino acid carrier system. *Cancer Res* 47:1571–1576
- Hawkins R, DeJoseph MR, Hawkins PA (1995) Regional brain glutamate transport in rats at normal and raised concentrations of circulating glutamate. *Cell Tissue Res* 281:207–214
- Hawkins RA, O'Kane RL, Simpson IA, Viña JR (2006) Structure of the blood–brain barrier and its role in the transport of amino acids. *J Nutr* 136(1):218–226
- Hellwig D, Gouverneur E, Schaefer A (2008) Para-[ $^{123}\text{I}$ ]iodo-L-phenylalanine in patients with pancreatic adenocarcinoma: tumour uptake, whole-body kinetics, dosimetry. *Nuklearmedizin* 47:220–224
- Holmboe L, Andersen AM, Mørkrød L (2012) High dose methotrexate chemotherapy: pharmacokinetics, folate and toxicity in osteosarcoma patients. *Br J Clin Pharmacol* 73:106–114
- Kersemans V, Cornelissen B, Bacher K (2005) In vivo evaluation and dosimetry of  $^{123}\text{I}$ -2-iodo-D-phenylalanine, a new potential tumor-specific tracer for SPECT, in an R1M rhabdomyosarcoma mouse model. *J Nucl Med* 46:2104–2111
- Laulloo SJ, Khodaboccus A, Hemraz U (2007) Use of Di-tert-butyl-dicarbonate both as a protecting and activating group in the synthesis of dipeptides. *Synth Commun* 37:4191–4197
- Martin B, Posseme F, Barbier CL (2002) (Z)-1,4-Diamino-2-butene as a vector of boron, fluorine, or iodine for cancer therapy and imaging: synthesis and biological evaluation. *Bioorg Med Chem* 10:2863–2871

- Muller M, dela Peria A, Derendorf H (2004) Issues in pharmacokinetics and pharmacodynamics of antifective agents: distribution to tissues. *Antimicrob Agents Chemother* 48:1441–1453
- Neuwelt EA, Diehl JT, Vu LH (1981) Monitoring of methotrexate delivery in patients with malignant brain tumors after osmotic blood–brain barrier disruption. *Ann Intern Med* 94:449–454
- Norrby SR (1985) Role of cephalosporins in the treatment of bacterial meningitis in adults. Overview with special emphasis on ceftazidime. *Am J Med* 79:56–61
- O'Brien P, Roos D, Pratt G (2000) Phase II multicenter study of brief single-agent methotrexate followed by irradiation in primary CNS lymphoma. *J Clin Oncol* 18:519–526
- Ozeki T, Hashizawa K, Kaneko D (2010) Treatment of rat brain tumors using sustained-release of camptothecin from poly(lactic-co-glycolic acid) microspheres in a thermoreversible hydrogel. *Chem Pharm Bull* 58:1142–1147
- Pardridge WM (2012) Drug transport across the blood–brain barrier. *J Cereb Blood Flow Metab* 32:1959–1972
- Peura L, Malmioja K, Huttunen K (2013) Erratum to: design, synthesis and brain uptake of lat1-targeted amino acid prodrugs of dopamine. *Pharm Res* 30:1714–1717
- Poulin P, Theil FP (2000) A priori prediction of tissue: plasma partition coefficients of drugs to facilitate the use of physiologically-based pharmacokinetic models in drug discovery. *Pharm Sci* 89:16–35
- Rajput N, Dumka VK, Sandhu HS (2012) Disposition kinetics and in vitro plasma protein binding of ceftiofime in cattle. *Vet Arhiv* 82:1–9
- Rao TS, Baker GB, Coutts RT (1987) *N*-(3-chloropropyl) phenylethylamine as a possible prodrug of beta-phenylethylamine: studies in the rat brain. *Prog Neuropsychopharmacol Biol Psychiatry* 11:301–308
- Reddy L, Sharma R, Chuttani K (2004) Etoposide-incorporated tripalmitin nanoparticles with different surface charge: formulation, characterization, radiolabeling, and biodistribution studies. *AAPS J* 6:55–64
- Samnack S, Romenik BF, Kubuschok B (2004) *p*-[123I]iodo-L-phenylalanine for detection of pancreatic cancer: basic investigations of the uptake characteristics in primary human pancreatic tumour cells and evaluation in in vivo models of human pancreatic adenocarcinoma. *Eur J Nucl Med Mol Imaging* 31:532–541
- Shingaki T, Inoue D, Furubayashi T (2010) Transnasal delivery of methotrexate to brain tumors in rats: a new strategy for brain tumor chemotherapy. *Mol Pharm* 7:1561–1568
- Simoes MF, Valente E, Gomez MJ (2009) Lipophilic pyrazinoic acid amide and ester prodrugs stability, activation and activity against *M. tuberculosis*. *Eur J Pharm Sci* 37:257–263
- Singhai AK, Jain S, Jain NK (1997) Evaluation of an aqueous injection of Ketoprofen. *Pharmazie* 52:149–151
- Stubblefield MD, Vahdat LT, Balmaceda CM, Troxel AB, Hesdorffer CS, Gooch CL (2005) Glutamine as a neuroprotective agent in high-dose paclitaxel-induced peripheral neuropathy: a clinical and electrophysiologic study. *Clin Oncol (R Coll Radiol)* 17(4):271–276
- Uchino H, Kanai Y, Kim DK, Wempe MF, Chairoungdua A, Morimoto E, Anders MW, Endou H (2002) Transport of amino acid-related compounds mediated by L-type amino acid transporter 1 (LAT1): insights into the mechanisms of substrate recognition. *Mol Pharmacol* 61:729–737
- Umapathy NS, Dun Y, Martin PM, Duplantier JN, Roon P, Prasad P, Smith SB, Ganapathy DV (2008) Expression and function of system N glutamine transporters (SN1/SN2 or SNAT3/SNAT5) in retinal ganglion cells invest. *Ophthalmol Vis Sci* 49(11):5151–5160
- Vyas TK, Babbar AK, Sharma RK (2006) Preliminary brain-targeting studies on intranasal mucoadhesive microemulsions of sumatriptan. *AAPS Pharm Sci Tech* 7:49–57
- Wang L, Qu W, Lieberman BP (2011) Synthesis, uptake mechanism, characterisation and biological evaluation of <sup>18</sup>F labeled fluoro-alkyl phenylalanine analogs as potential PET imaging agents. *Nucl Med Biol* 38:53–62
- Widemann BC, Adamson PC (2006) Understanding and managing methotrexate nephrotoxicity. *Oncologist* 11:694–703
- Widemann BC, Sung E, Anderson L (2000) Pharmacokinetics and metabolism of the methotrexate metabolite, 2,4-diamino-N<sup>10</sup>-methylptericoic acid. *J Pharmacol Exp Ther* 294:894–901
- Wu G, Barth RF, Yang W (2006) Targeted delivery of methotrexate to epidermal growth factor receptor–positive brain tumors by means of cetuximab (IMC-C225) dendrimer bioconjugates. *Mol Cancer Ther* 5:52–59
- Zhou K, Khokhar JY, Zhao B (2013) First demonstration that brain CYP2D-mediated opiate metabolic activation alters analgesia in vivo. *Biochem Pharmacol* 85:1848–1855